



**IIS** – ISTITUTO ITALIANO DELLA SALDATURA – ENTE MORALE  
LABORATORIO

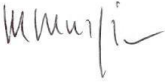
**Tested for you...**

**HyperFill™ technology of Lincoln Electric**

**Document** LSP/LAS/051L.20  
**Rev.** 1  
**Client** Lincoln Electric Srl  
**Job number** I00003107.01

*This document may not be partially reproduced, unless approved in writing  
The results contained in this document refer only to the objects tested*

---

<b>Written</b>	<b>Checked</b>	<b>Visa</b>	<b>Approved</b>	<b>Date</b>
Alessio Bazzurro	Matteo Pedemonte		Michele Murgia	
				21/05/2020

## INDEX

1	PRESENTATION OF THE PRODUCT .....	3
2	REALIZATION OF THE JOINTS .....	5
2.1	BASE AND FILLER MATERIALS .....	5
2.2	Welding configuration and process parameters .....	6
3	TESTS CARRIED OUT .....	9
3.1	Corner joints.....	9
3.2	Butt joints .....	13
4	CONCLUSIONS .....	19
5	REFERENCES .....	21

## 1 PRESENTATION OF THE PRODUCT

The Focus of the rubric “Tested for you” of this number of the Italian Welding Magazine is the HyperFill™ technology developed by Lincoln Electric, American Company that have his core business in the design, development and manufacture of arc welding products, automated joining, assembly and cutting systems, plasma and oxy-fuel cutting and brazing and soldering alloys.

Will be now introduced the aforesaid technology, whose characteristic can be easily found on the brochure downloadable on the site [www.lincolnelectric.com](http://www.lincolnelectric.com).

HyperFill™ is a patented twin-wire GMAW-P solution that utilizes two electrically conductive wires, energized by a single power source and fed through a single wire feeder, single gun liner and a single tip.

A panoramic view of welding generator and equipment (specifically that used in this analysis) is reported in fig. 1.1.



Fig. 1.1 – Welding generator and equipment for HyperFill™ technology

By substituting two smaller diameter wires in place of a single large diameter wire, the HyperFill™ process increases the droplet size and spreads out the arc cone (one single arc is originated), allowing for improved deposition rates while maintaining arc stability. The result is a process that increases the usable deposition rates of GMAW while making it simpler for the welder or the operator to manage a large weld puddle. Compared to traditional single wire processes, productivity can be increased up to 50% or more.

Another feature is the fact that the orientation of the two wires, compared to the welding direction of the joint, does not affect the characteristics of the arc even less the shape/size of the bead contrary to what happens for tandem processes. In addition, in the welding of corner joints in the frontal plane (PB), the ability to generate single-pass fillet weld characterized by throat thicknesses greater than 7 mm together with maintaining the symmetry of the geometric profile of the bead is highlighted.

It should be noted that the process, in addition to being used in a partly mechanised mode, can be extended to automated and robotic applications or with portable welding tractors.

As previously said, it is a pulsed welding process, whose characteristic waveform is reported in figure 1.2. As current increases from background to peak, the ends of the wire become hot, start to become liquid, and the magnetic fields around the wires, push the liquid into a common droplet, forming a “liquid bridge” (phase 1). The high and the long peak current apply pinch force to the liquid bridge droplet pushing it toward the weld pool and separating it from the consumable wires (phase 2). The slow tailout completes separation of the droplet toward the weld pool (phase 3). The background maintains the arc, supplies heat to the weld pool, and allows the wire feeder to advance wire making it ready to transfer the next droplet (phase 4).

As our readers well know, the purpose of this rubric is not to endorse or deny what is reported by the manufacturer, but to test the process object of the analysis by means of a series of quantitative and qualitative tests, which will be described in the following paragraphs.

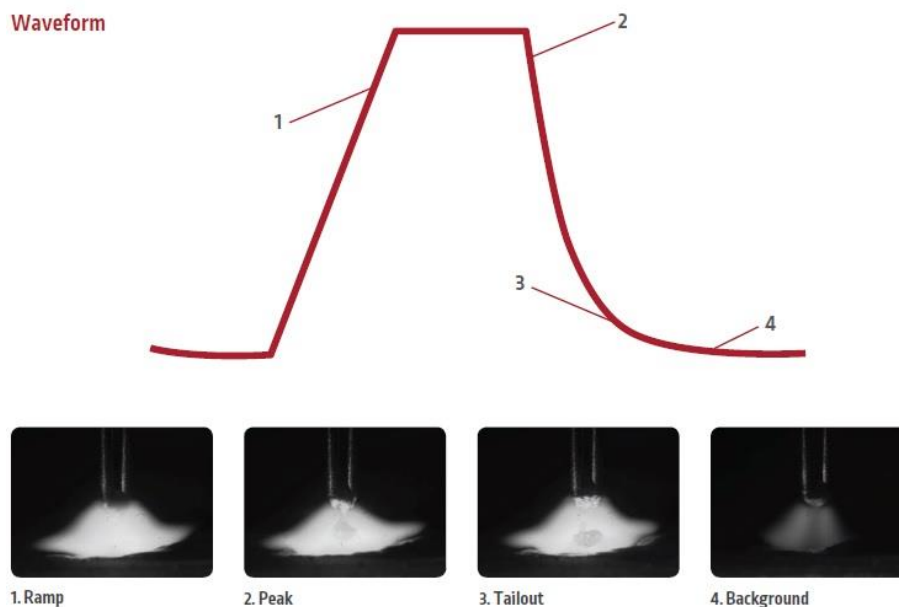


Fig. 1.2 – Characteristic waveform of HyperFill™ process

## 2 REALIZATION OF THE JOINTS

The test plan was based on the comparison between the HyperFill™ process and the traditional single wire GMAW process by manufacturing, for each type of process, a full penetration butt joint and a corner joint on which the following tests were conducted:

- radiographic testing (butt joints), according to UNI EN ISO 17636-2;
- penetrant testing (butt joints and fillet weld), according to UNI EN ISO 3452-1;
- macroscopic examination (butt joints and fillet weld), according to UNI EN ISO 17639;
- vickers hardness test (butt joints and fillet weld), according to UNI EN ISO 6507-1;
- tensile test (butt joints), according to UNI EN ISO 6892-1;
- bend test (butt joints), according to UNI EN ISO 5173;
- charpy impact test (butt joints), according to UNI EN ISO 148-1.

These tests follow the qualification process of the UNI EN ISO 15614-1 standard, although it should be noted that the processes in the article have not been subjected to a real process of qualification of the procedure.

The samples were realized at the Lincoln Electric facilities in Rivoli Veronese (VR), in the presence of IIS staff. The tests were carried out at the Laboratory of the Italian Institute of Welding.

### 2.1 BASE AND FILLER MATERIALS

20 mm thick UNI EN ISO 10025-2 S355J2 carbon steel was chosen as the base material. While as regards the filler material, the choice fell on Lincoln Electric SupraMig® HD consumable classified as ER70S-6 according to the AWS A5.18 standard, and G42 3 C 3Si1 / G46 4 M 3Si1 in accordance with UNI EN ISO 14341-A.

A pair of 1,0 mm wires was used for the HyperFill™ process while a 1,2 mm wire was used for the GMAW.

Chemical compositions of aforesaid materials are reported in table 1 and table 2.

Lincoln Electric SupraMig® HD			
%C	%Mn	%Si	%Fe
0,08	1,40	0,85	Balance

Table 1 – Chemical composition of filler material

UNI EN ISO 10025-2 S355J2													
%C	%Si	%Mn	%P	%S	%Cr	%Ni	%Cu	%Al	%Nb	%V	%N	%Ti	%Fe
0,19	0,21	1,44	0,013	0,006	0,03	0,01	0,02	0,034	0,009	0,004	0,007	0,004	Bal.

Table 2 – Chemical composition of base material

## 2.2 Welding configuration and process parameters

Table 3 shows the welding configurations adopted.

	GMAW	HyperFill™
Generator	Power Wave® S500 C	Power Wave® S500 C
Wire feeder	Power Feed® 46	Power Feed® 84
Torch	LGS2 505 W-4.0M	Magnum® PRO 500W

Table 3 – Welding configurations adopted

The samples were realized by adopting a mechanized torch movement system in order to limit the variations of the process parameters and increase their repeatability; Figure 2.2.1 shows the torch positioning adjustment phase during the realization of one of the butt joints. Figure 2.2.2 schematizes the preparation of the joint adopted for this type of junctions, the same for both processes. A ceramic support plate type KERALINE TA2 was used.



Fig. 2.2.1 – Fit-up of the butt joint

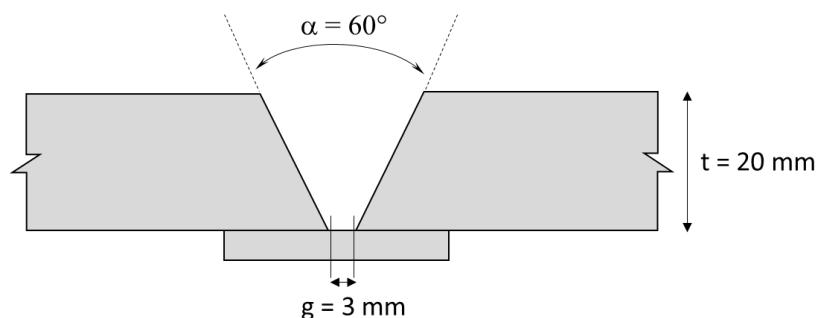


Fig. 2.2.2 – Scheme of the preparation of the butt joints

The process parameters adopted and the calculation of the heat input in accordance with UNI EN 1011-1 are reported in tables 4, 5, 6 and 7. An Ar (84%) - CO<sub>2</sub> (16%) mixture was used as the shielding gas, identified with the code M21 according to UNI EN ISO 14175. The tests were carried out without preheating with an interpass temperature of 150°C.

Bead No	Arc voltage [V]	Current [A]	Wire speed [m/min]	Feed rate [mm/min]	Stick-out [mm]	Shielding gas flow rate [l/min]	Heat input [kJ/mm]
1	28,5±0,2	280±5	9	250	20	15÷20	1,53
2	28,5±0,2	280±5	9	250	20	15÷20	1,53
3	28,5±0,2	280±5	9	300	20	15÷20	1,28
4	28,5±0,2	280±5	9	300	20	15÷20	1,28
5	28,5±0,2	290±5	9	300	20	15÷20	1,32
6	28,5±0,2	290±5	9	300	20	15÷20	1,32
7	28,5±0,2	280±5	9	300	20	15÷20	1,28
8	28,5±0,2	275±5	9	300	20	15÷20	1,25
9	28,5±0,2	285±5	9	350	20	15÷20	1,11

Table 4 – GMAW: butt joint process parameters

Bead No	Arc voltage [V]	Current [A]	Wire speed [m/min]	Feed rate [mm/min]	Stick-out [mm]	Shielding gas flow rate [l/min]	Heat input [kJ/mm]
1	28,5±0,2	275±5	9	250	20	15÷20	1,50

Table 5 – GMAW: corner joint process parameter

Bead No	Arc voltage [V]	Current [A]	Wire speed [m/min]	Feed rate [mm/min]	Stick-out [mm]	Shielding gas flow rate [l/min]	Heat input [kJ/mm]
1	32±0,2	375±5	11	300	25	25÷30	1,92
2	32±0,2	385±5	11	300	25	25÷30	1,97
3	32±0,2	390±5	11	390	25	25÷30	1,54
4	32±0,2	385±5	11	390	25	25÷30	1,52
5	32±0,2	375±5	11	390	25	25÷30	1,48
6	32±0,2	355±5	11	390	25	25÷30	1,40

Table 6 – HyperFill™: butt joint process parameter

Bead No	Arc voltage [V]	Current [A]	Wire speed [m/min]	Feed rate [mm/min]	Stick-out [mm]	Shielding gas flow rate [l/min]	Heat input [kJ/mm]
1	32±0,2	370±5	11	380	25	25÷30	1,50

Table 7 – HyperFill™: corner joint process parameter

An analysis of the tables shows the higher values of the electrical parameters (with current intensities of about 400 A) and consequently of the forward speed that characterize the HyperFill™ process compared to a traditional GMAW. The gas flow rate also needs to be increased, as well as the stick-out, which must be set around 25 mm to ensure correct interaction between the two wires (fig. 2.2.3).

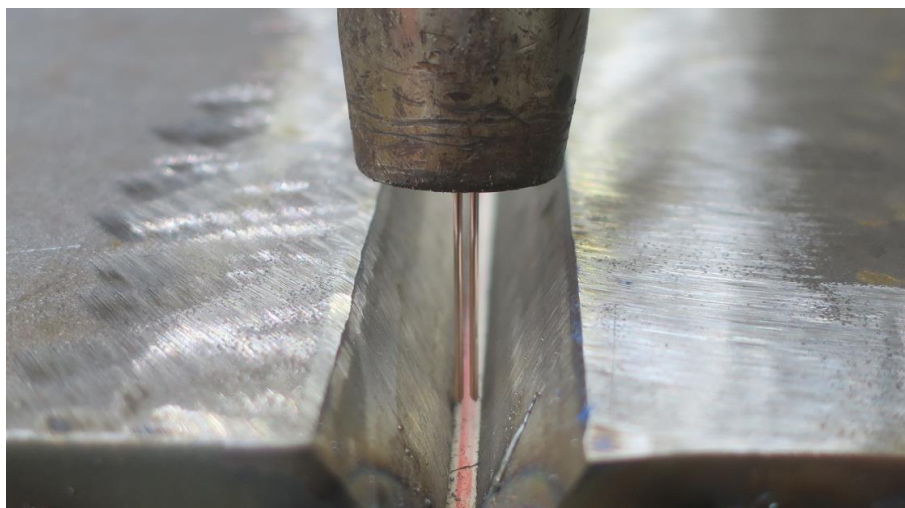


Fig. 2.2.3 – Detail of the twin-wire in HyperFill™ process

Regarding the wire feed speed, this has a minimum operating value of the order of 8.5 m/min with an optimal value between 10 and 11 m/min.

Figures 2.2.4 and 2.2.5 show the four samples realized.



Fig. 2.2.4 – Joints realized with HyperFill™ process



Fig. 2.2.5 – Joints realized with GMAW process

### 3 TESTS CARRIED OUT

The following paragraphs describe in detail the results of the tests carried out, divided by type of joint.

#### 3.1 Corner joints

##### Non destructive testing

Penetrant testing did not reveal surface discontinuities in either of the two controlled joints. As an example, figure 3.1.1 shows the control conducted on the fillet welds of the HyperFill™ process.

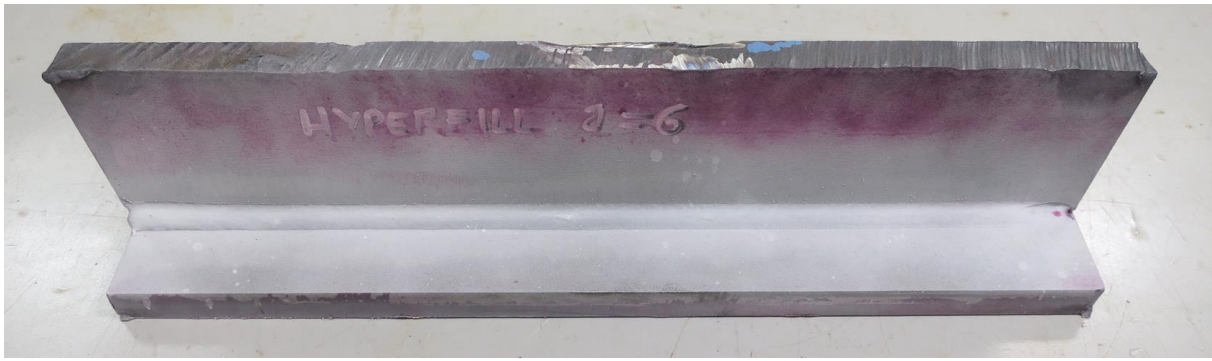


Fig. 3.1.1 – PT on fillet weld realized with HyperFill™

### Macroscopic examination

Four macrographic sections were taken from the corner joints (two per joint), two of which are shown in figures 3.1.2 and 3.1.3. The chemical attack was carried out with a 10% Nital-based solution. As documented by the macrographs, for the same throat thickness (the values of which are shown in table 8), it is noted that in the corner joint made with the HyperFill™ process the cross sections of the beads have more uniform profile with more limited shape variations.

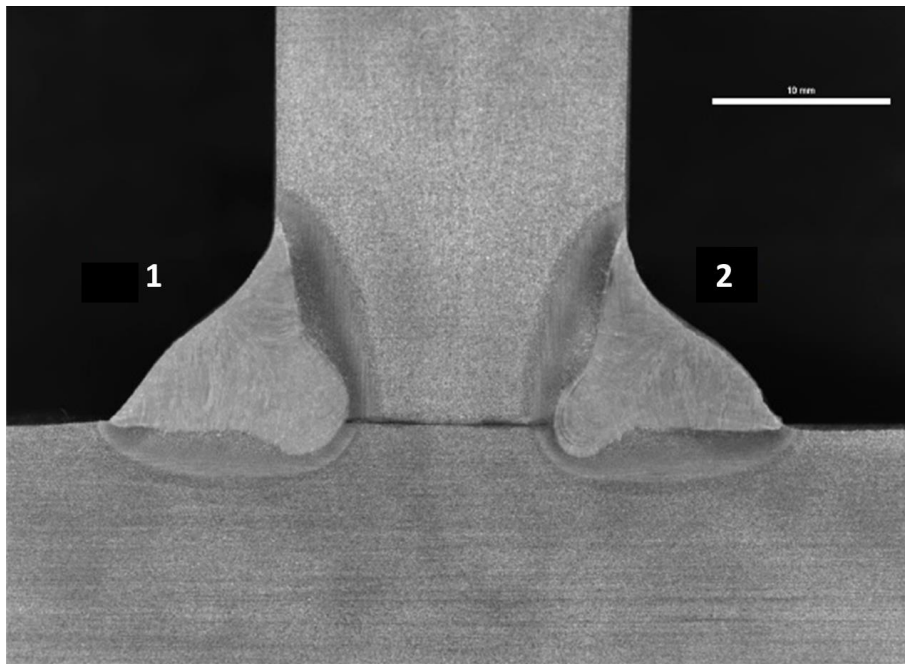


Fig. 3.1.2 – Macrographic section of the corner joints realized with GMAW

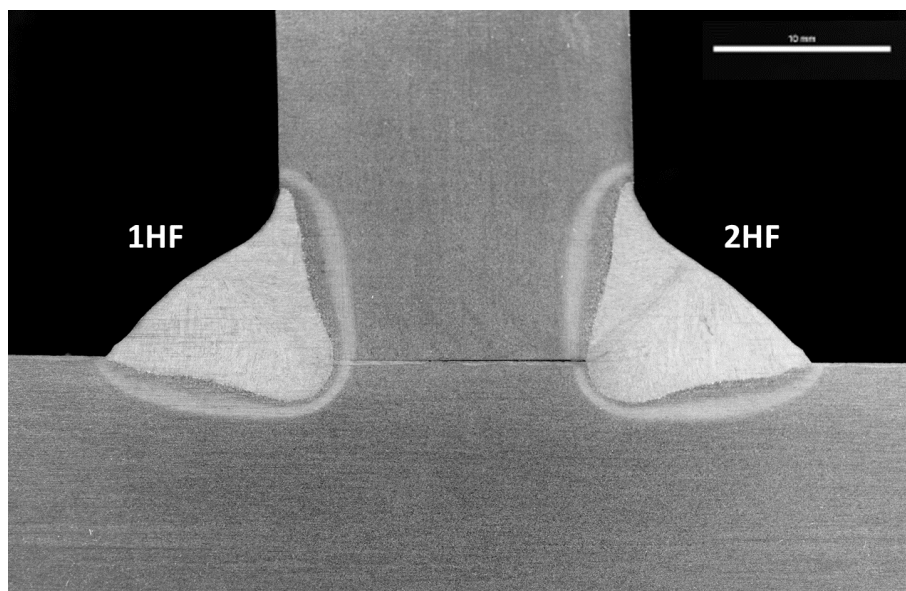


Fig. 3.1.3 – Macrographic section of the corner joints realized with HyperFill™

GMAW		HyperFill™	
Section 1	Section 2	Section 1HF	Section 2HF
6.20 mm	6.00 mm	6.40 mm	6.45 mm

Table 8 – Throat thickness of the fillet weld

#### Vickers hardness test (HV10)

Figure 3.1.4 shows the measurement scheme of the HV10 indentations, while the trend of the hardness profile is shown in the graph in Figure 3.1.5; for values, see table 9.

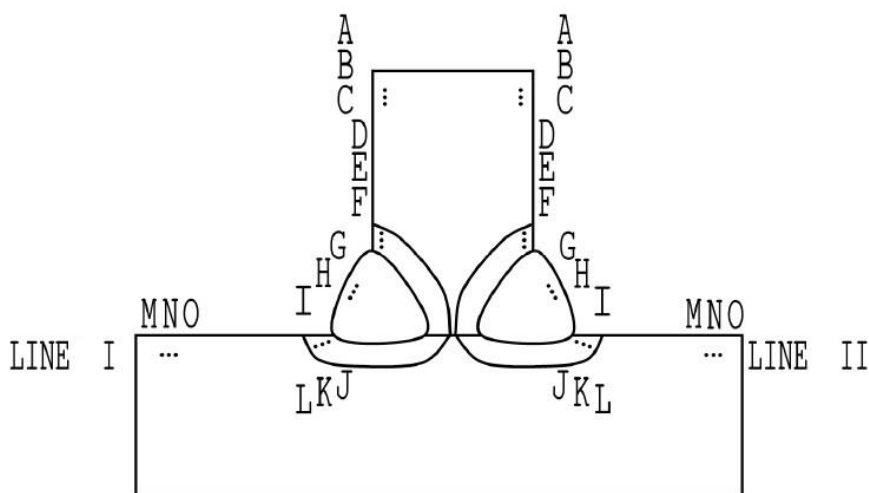
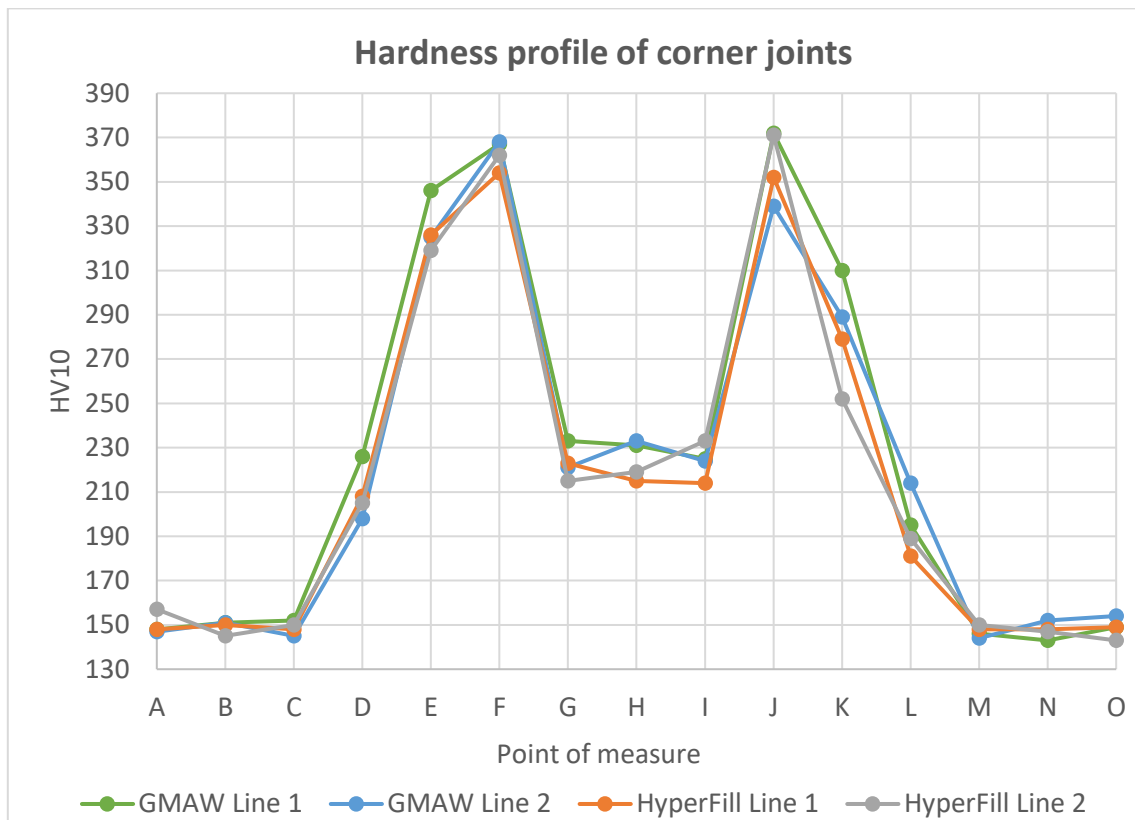


Fig. 3.1.4 – Scheme of HV10 indentations



*Fig. 3.1.5 – Trend of hardness profile observed in corner joints*

Measurement area	GMAW Line 1	GMAW Line 2	HyperFill Line 1	HyperFill Line 2
A (BM)	148	147	148	157
B (BM)	151	151	150	145
C (BM)	152	145	148	150
D (HAZ)	226	198	208	205
E (HAZ)	346	325	326	319
F (HAZ)	367	368	354	362
G (MZ)	233	221	223	215
H (MZ)	231	233	215	219
I (MZ)	225	224	214	233
J (HAZ)	372	339	352	371
K (HAZ)	310	289	279	252
L (HAZ)	195	214	181	189
M (BM)	146	144	148	150
N (BM)	143	152	148	147
O (BM)	149	154	149	143

*Table 9 – Hardness values (corner joints)*

Looking at the graph in figure 3.1.5, it is highlighted that, in the two processes, the values obtained as well as the trend observed do not show evident differences. The measurements made on the base material show hardness values between 143 and 157 HV. The highest values were recorded in the heat affected zone (HAZ), with a peak of 372 HV in the GMAW process and a maximum of 371 with HyperFill™ technology. In the molten zone (MZ) with both processes the hardness does not exceed 233 HV.

Tables 5 and 7 show that the heat input generated by the two processes for making fillet welds is the same, consequently there are no marked differences between the hardness profiles. However, at equal throat thickness, the HyperFill™ process allows to reduce the execution times of the pass by increasing the feed speed by 52% compared to that adopted with the GMAW single wire process.

### 3.2 Butt joints

#### Non destructive testing

The penetrant testing did not detect surface discontinuities in either of the two controlled joints. As an example, figure 3.2.1 shows the control conducted on the butt joint of the HyperFill™ process.



Fig. 3.2.1 – Liquid penetrant inspection on HyperFill™ butt joint

At a volumetric level, the radiographic examination has identified the presence of gas pores, mainly in the joint made with GMAW, in which they are uniformly distributed; figure 3.2.2 shows the radiographic films of the two butt joints.

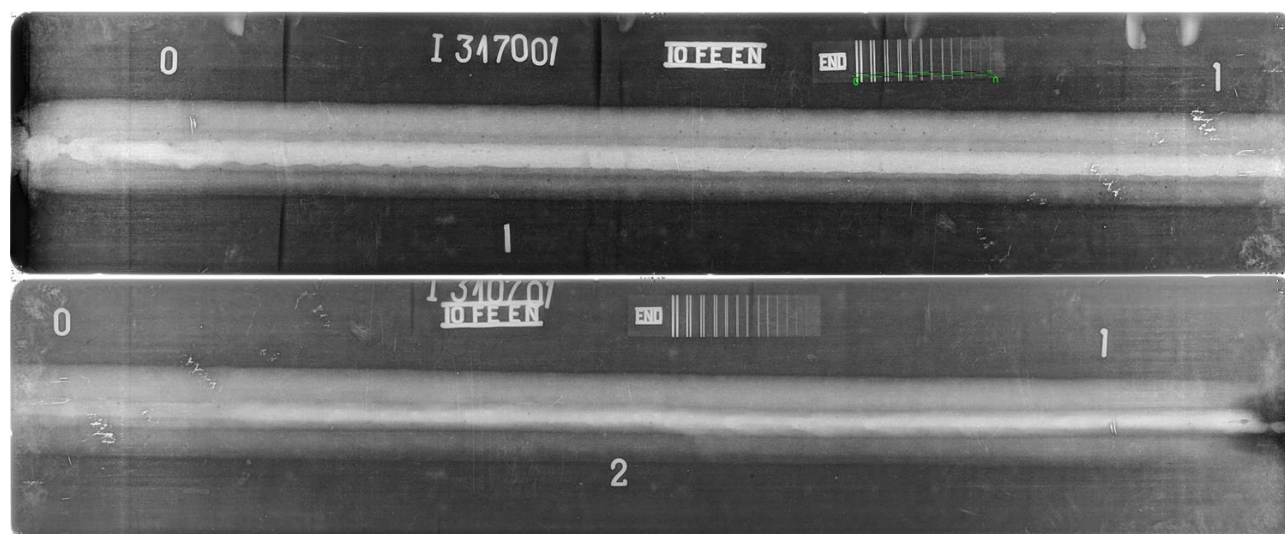


Fig. 3.2.2 – Radiographic film of the butt joints: GMAW (above), HyperFill™ (below)

### Macroscopic examination

The macrographic sections taken from the butt joints are reported in figures 3.2.3 and 3.2.4. It can be seen that one of the major features of HyperFill™ technology, that means the high deposit rate, allows to reduce the number of passes compared to the GMAW process; specifically, 6 passes of the HyperFill™ process were sufficient for filling the welding gap compared to 9 passes of the traditional continuous wire process.

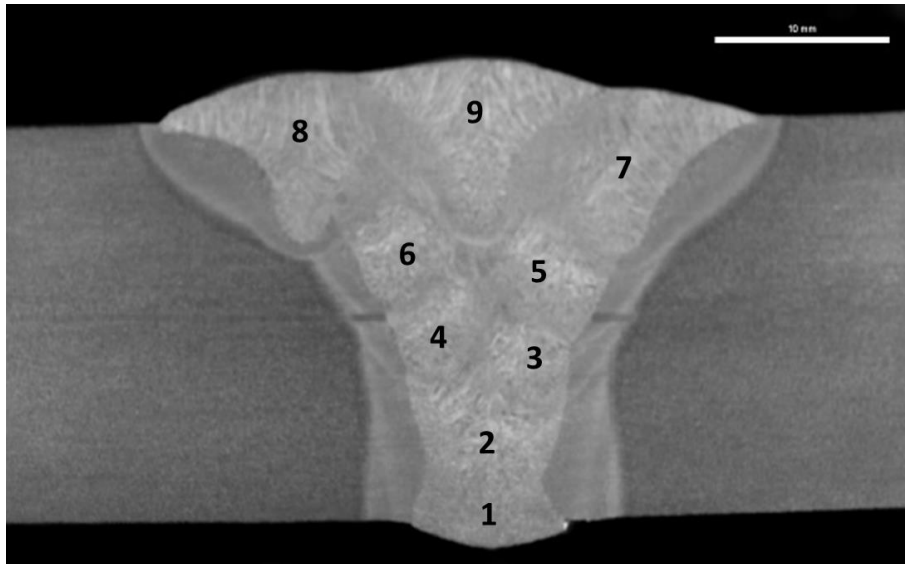


Fig. 3.2.3 – Macrographic section of the butt joint realized with GMAW

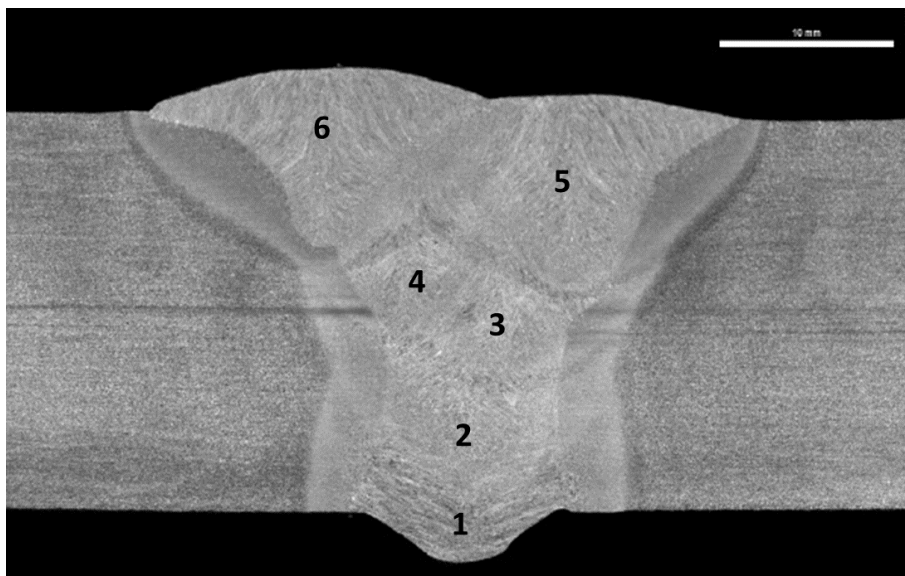


Fig. 3.2.4 – Macrographic section of the butt joint realized with HyperFill™

### Vickers hardness test (HV10)

Figure 3.2.5 shows the measurement scheme of the HV10 indentations, as regards the trend of the hardness profiles this is shown in the graph in Figure 3.2.6; for values, see table 10. From the hardness profiles in Line 1, it is observed that the joints made with the HyperFill™ process generally have lower values; specifically in the HAZ of the GMAW single wire process, a peak of 301 HV was measured while the maximum value reached in the HyperFill™ process is 261 HV. Molten zones have similar values of the order of 200 HV.

As regards line 2, also in this case the hardness of the joint made with the Hyperfill™ process generally has lower values, with a maximum of 199 HV in the measurement area F.

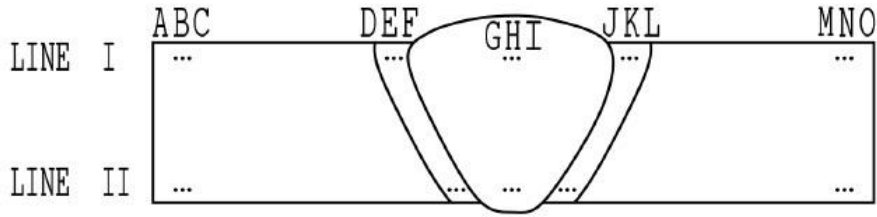


Fig. 3.2.5 – Scheme of HV10 indentations

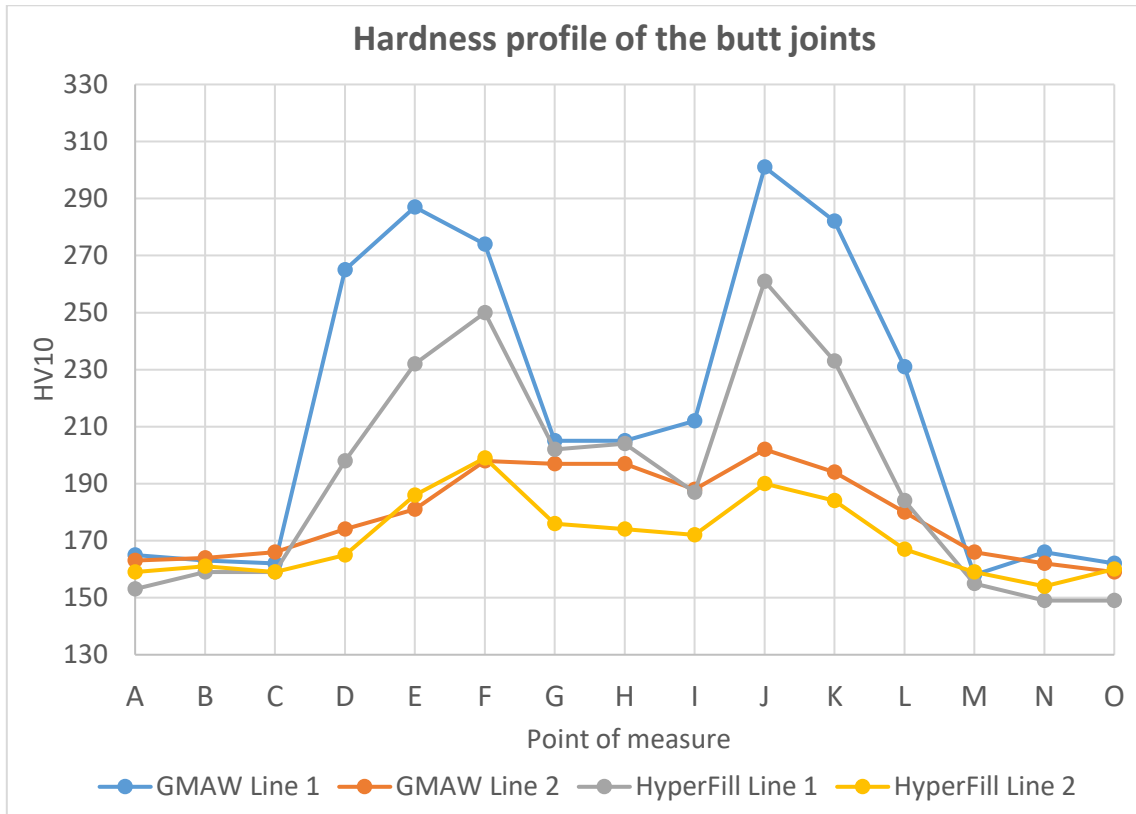


Fig. 3.2.6 – Trend of hardness profile observed in butt joints

Measurement area	GMAW Line 1	GMAW Line 2	HyperFill Line 1	HyperFill Line 2
A (BM)	165	163	153	159
B (BM)	163	164	159	161
C (BM)	162	166	159	159
D (HAZ)	265	174	198	165
E (HAZ)	287	181	232	186
F (HAZ)	274	198	250	199
G (MZ)	205	197	202	176
H (MZ)	205	197	204	174
I (MZ)	212	188	187	172
J (HAZ)	301	202	261	190
K (HAZ)	282	194	233	184
L (HAZ)	231	180	184	167
M (BM)	158	166	155	159
N (BM)	166	162	149	154
O (BM)	162	159	149	160

Table 10 – Hardness values (butt joints)

### Tensile test

Table 11 shows the results of the tensile tests carried out on transversal specimens. With both processes, the tensile strength obtained are close to 540 MPa, value that characterizes the base material used. As can be seen in figure 3.2.7, in all the specimens the fracture occurred in the base material.

	Specimen	Tensile strength [MPa]	Break point
GMAW	1	547	Base Material
	2	541	Base Material
HyperFill™	1HF	538	Base Material
	2HF	538	Base Material

Table 11 – Results of tensile test



Fig. 3.2.7 – Tested specimens

### Bend test

In the lateral bend tests four specimens were taken per sample and subjected to lateral bending with an angle of 180°. The results gave satisfactory outcome with both processes, not showing triggers of discontinuities related to operational problems such as lack of fusion. In figure 3.28 it is possible to observe the tested specimens.



Fig. 3.28 – Specimens submitted to lateral bend test: GMAW on the left, HyperFill™ on the right

### Charpy impact test

The Charpy impact tests were carried out at a temperature of -20 °C on specimens with V-notch made in the direction of the thickness; three specimens were taken in the heat affected zone and three in correspondence of the molten zone. The results, observable in table 12, also in this case are positive. The HyperFill™ process, compared to the test carried out with GMAW, shows a better behavior in HAZ but loses some Joule in the MZ.

	Specimen	Position	Temperature [°C]	Energy [J]	Average [J]
GMAW	1_F1	MZ	-20	128	104
	1_F2			95	
	1_F3			88	
	1_A1	HAZ		63	72
	1_A2			91	
	1_A3			64	
HyperFill™	2_F1	MZ		83	89
	2_F2			93	
	2_F3			91	
	2_A1	HAZ		78	87
	2_A2			91	
	2_A3			91	

Table 12 – Results of Charpy test

Additional test: fillet weld with 7 mm throat thickness

Finally, a further corner joint was carried out in order to evaluate the ability of HyperFill™ to create fillet weld in a single pass with throat thickness of 7 mm characterized by maintaining the symmetry of the geometric profile of the bead.

Figure 3.29 shows the macrographic section of the corner joint and table 13 reports throat thickness and leg length. As can be observed from the macrographic section and from the measured geometric parameters, the beads have symmetrical profile with reduced tendency to assume concavity in the upper part of the seam.

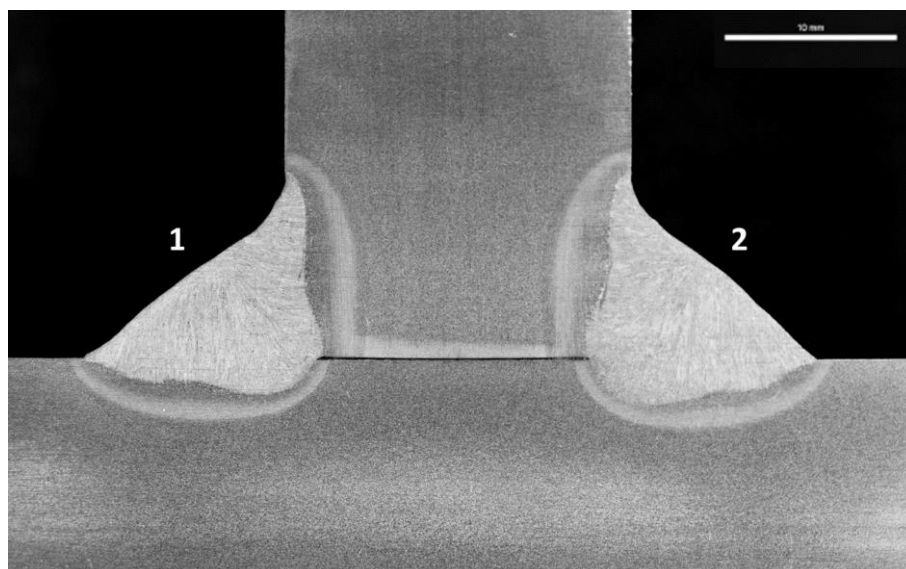


Fig. 3.29 – Macrographic section of the fillet weld with 7 mm throat thickness

	Section 1	Section 2
<b>Throat thickness</b>	7.00 mm	6.8 mm
<b>Leg length</b>	10,5x11,3 mm	10,5x10,6 mm

Table 13 – Throat thickness and leg length

## 4 CONCLUSIONS

The main aspects that emerged from the comparison between the two processes will be commented below. For the convenience of the reader, it is considered useful to summarize the main aspects of the individual tests in the following tables.

Corner joints	
<b>NDT (PT)</b>	Surface inspection with penetrating liquids revealed no indications.
<b>Macroscopic examination</b>	At the same throat thickness, fillet weld made with the HyperFill™ process have more uniform profile with more limited shape variations.
<b>Vickers hardness HV 10</b>	The hardness profiles of the joints made with the two processes do not show marked differences. This can be attributed to the fact that the heat input used to make the joints was found to be the same in both cases. In fact, the high electrical parameters used in the HyperFill™ process are balanced by the equally high forward speed.

*Table 14 – Summary corner joints test*

Butt joints	
<b>NDT (PT and RT)</b>	Surface inspection with penetrating liquids revealed no indications. The volumetric control detected porosity in both samples; more markedly with the GMAW.
<b>Macroscopic examination</b>	With the same joint preparation, the reduction of the number of passes necessary for filling the welding gap can be observed; from 9 in the GMAW process to 6 in the HyperFill™ technology. In the first two passes (lower part of the macrographic section), with the latter process, there was a greater extension of the MZ and HAZ, considered the greater heat input adopted (about 0,4 kJ more). The dimensions become comparable in the upper part of the joint, reducing the gap between the heat input of the two processes.
<b>Vickers hardness HV 10</b>	Consequently to the milder thermal cycle, the trend of the hardness profiles in the HyperFill™ process is generally more contained.
<b>Tensile test</b>	With both processes, the test gave a positive result and there are no obvious differences. In all the specimens the fracture occurred in base material.
<b>Bend test</b>	The results gave satisfactory outcome with both processes, not showing discontinuity triggers related to operational problems.
<b>Charpy impact test</b>	With HyperFill™ technology there is a small difference between the values obtained in MZ and HAZ. Compared to the GMAW process, the specimens picked up in HAZ has slightly higher resilience; this behaviour reverses in correspondence of the MZ.

*Table 15 – Summary butt joint test*

### Considerations about productivity

We want to conclude the article by making some considerations of operative nature in relation to the characteristics of productivity.

In butt joints by adding the times of realization of the single beads, calculated considering as input data the length of the passes (550 mm) and the speed of realization of these (see tables 4 and 6), the following switched on arc durations are obtained:

- 17 minutes for GMAW process;
- 9,3 minutes for HyperFill™ technology.

By schematizing the volume of filler material deposited (fig. 4.1) as the sum of the volume occupied by the welding gap plus that of the excess of weld metal on the surface and the root, it is obtained a value of about 0.18 dm<sup>3</sup>. Table 16 shows the value of the individual areas, calculated from the geometric parameters of the chamfer.

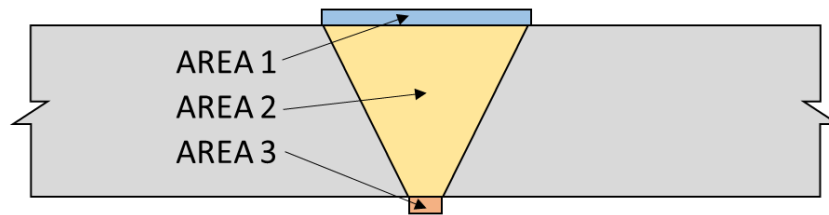


Fig. 4.1 – Schematization of the surface occupied by the filler material

AREA 1	AREA 2	AREA 3
291 mm <sup>3</sup>	39,15 mm <sup>3</sup>	4,5 mm <sup>3</sup>
a) 1,5 mm of excess of weld metal was adopted both to the top and to the root		
b) Length of the plates: 550 mm		

Table 16 – Valore delle aree calcolate a partire dai parametri geometrici del cianfrino

Considering a density of the filler material equal to 7,8 kg/dm<sup>3</sup>, the use of approximately 1,4 kg of consumable are calculated; this amount of material is deposited in 9,3 minutes with Hyperfill™ technology and in 17 minutes with the GMAW process.

Taking 60 minutes as the reference value and making the due proportions, the following deposit rate are reached:

- about 5 kg/h (GMAW);
- about 9 kg/h (HyperFill™).

So in the tests conducted, the technology developed by Lincoln Electric has proven to be able to significantly increase productivity by combining high feed rates together with high deposit rates using twin-wire technology and pulsed process.

## 5 REFERENCES

- [1] UNI EN ISO 15614-1:2017 – “Specifica e qualificazione delle procedure di saldatura per materiali metallici – Prove di qualificazione della procedura di saldatura – Parte 1: Saldatura ad arco e a gas degli acciai e saldatura ad arco del nichel e sue leghe”
- [2] UNI EN ISO 17636-2:2013 – “Controllo non distruttivo delle saldature. Controllo radiografico dei giunti saldati”
- [3] UNI EN ISO 3452-1 - “Prove non distruttive. Esame con liquidi penetranti. Parte 1: Principi generali”
- [4] UNI EN ISO 17639:2013 – “Prove distruttive sulle saldature di materiali metallici. Esame microscopico e macroscopico dei giunti saldati”
- [5] UNI UN ISO 6507-1:2018 – “Materiali metallici – Prova di durezza Vickers – Parte 1: Metodo di prova”
- [6] UNI EN ISO 6892-1:2016 – “Materiali metallici – Prova di trazione. Parte 1: Metodo di prova a temperatura ambiente”
- [7] UNI EN ISO 5173:2012 – “Prove distruttive sulle saldature di materiali metallici: prova di piegamento”
- [8] UNI EN ISO 148-1:2016 – “Materiali metallici. Prova di resilienza su provetta Charpy. Parte 1: Metodo di prova”
- [9] Prodotti laminati a caldo di acciai per impieghi strutturali – Parte2: Condizioni tecniche di fornitura di acciai non legati per impieghi strutturali”
- [10] AWS A5.18 – “Specification for carbon steel electrodes and rods for gas shielded arc welding”
- [11] UNI EN ISO 14341 – “Materiali di apporto per saldatura – Fili elettrodi e depositi per saldatura ad arco in gas protettivo di acciai non legati e a grano fine – Classificazione”
- [12] UNI EN ISO 17637 - “Controllo non distruttivo delle saldature. Esame visivo dei giunti saldati per fusione”
- [13] ISO 5817 - “Welding - Fusion-welded joints in steel, nickel, titanium and their alloys (beam welding excluded) - Quality levels for imperfections”
- [14] UNI EN ISO 6520 – “Saldatura e procedimenti connessi – Classificazione delle imperfezioni geometriche nei materiali metallici”
- [15] UNI EN1011-1 – “Saldatura – Raccomandazioni per la saldatura di materiali metallici – Parte 1 Guida generale per la saldatura ad arco”

Unless otherwise specified, the cited documents were applied in the valid edition on the date of writing of this document.